Linear anhysteretic direct magnetoelectric effect in $Ni_{0.5}Zn_{0.5}Fe_2O_4$/poly(vinylidene fluoride-trifluoroethylene) 0-3 nanocomposites

P. Martins[1], X. Moya[2], L. C. Phillips[2], S. Kar-Narayan[2], N. D. Mathur[2] and S. Lanceros-Mendez[1]

[1]Centro/Departamento de Física, Universidade do Minho, 4710-057, Braga, Portugal

[2]Department of Materials Science, University of Cambridge, Cambridge, CB2 3QZ, United Kingdom

Abstract

Free-standing flexible magnetoelectric 0-3 composite films, comprising $Ni_{0.5}Zn_{0.5}Fe_2O_4$ (NZFO) ferrite nanoparticles in a poly(vinylidene fluoride-trifluoroethylene) [P(VDF-TrFE)] copolymer matrix, have been prepared at low temperatures by solvent casting and melt crystallization. Ferroelectric, piezoelectric, magnetic and direct magnetoelectric properties of the nanocomposites depend strongly on ferrite concentration. Magnetoelectric voltage coefficients increase linearly with applied dc magnetic-bias fields up to 5 kOe and show no hysteresis. At this field, a maximum magnetoelectric voltage coefficient of 1.35 mV cm^{-1} Oe^{-1} was obtained for samples with 15 wt. % ferrite using a 40 kHz resonant signal.

PACS: 75.85.+t, 77.55.Nv, 75.75.Fk, 77.65.-j, 75.80.+q, 75.50.Gg, 77.80.-e

Keywords: magnetoelectric, polymer composites, elecroactive polymers

Introduction

Magnetoelectric effects arise in materials, or combinations of materials, that are electrically and magnetically polarizable due to coupling between electrical polarization and magnetization mediated sometimes by strain[1]. The direct magnetoelectric effect is the modification of electrical polarization *P* by magnetic field *H*, and the converse effect is the change of magnetization *M* by electric field *E*. Intrinsic magnetoelectric effects in single-phase materials typically occur at low temperatures and are weak[1,2]. Two-phase composites consisting of strain-coupled piezoelectric (or electrostrictive) and magnetostrictive (or piezomagnetic) materials yield large magnetoelectric effects at room temperature[3] and are therefore interesting for applications, e.g. magnetic-field sensors, transducers, resonators and energy harvesting[3,4].

The performance of magnetoelectric composites depends both on the piezoelectric (or electrostrictive) and magnetostrictive (or piezomagnetic) properties of the individual components and their coupling. Strain coupling requires intimate contact between the constituent phases and depends strongly on the geometry of the composite, which is usually described by the connectivity of the phases. Giant direct magnetoelectric voltage coefficients, $\alpha \sim 7$ V cm^{-1} Oe^{-1} at low frequencies and ~ 300 V cm^{-1} Oe^{-1} at the 50 kHz resonance, have been reported in 2-2 laminate composites of high-magnetic-permeability Fe-Si-Co Metglas and piezoelectric polyvinylidene fluoride (PVDF) polymer layers bonded using epoxy resin[5]. Similar values have been observed in 2-1 laminate composites consisting of piezoelectric Pb(Zr,Ti)O_3 fibres bonded between Fe-B-Si-C Metglas layers using epoxy resin[6], ~ 20 V cm^{-1} Oe^{-1} at low frequencies and ~ 750 V cm^{-1} Oe^{-1} at the 21 kHz resonance.

The strong magnetoelectric effects discussed above are non-linear and occur only at low magnetic bias fields (< 20 Oe) such that they are not suitable for use as high-field dc magnetic sensors. Moreover, performance is compromised by the relative brittleness of the epoxy bonding the component phases. However, 0-3 composites of magnetic nanoparticles embedded in a ferroelectric polymer matrix overcome this problem because the magnetic material is in direct contact with, and completely surrounded by, the ferroelectric material. Also, for sufficiently small nanoparticle weight fractions, the mechanical properties of the ferroelectric polymer are preserved and therefore the nanocomposites can be easily processed at low temperatures into a variety of shapes for applications[3,7].

Recently, small magnetoelectric effects up to 40 mV cm^{-1} Oe^{-1} were obtained in $CoFe_2O_4$/P(VDF-TrFE) nanocomposites[7] at high dc magnetic bias fields (2 kOe). However, the magnetoelectric response was found to be non-linear at these high fields, and hysteretic at lower fields ($CoFe_2O_4$ nanoparticles have coercive field H_c = 1.4 kOe), precluding applications. Here we exploit $Ni_{0.5}Zn_{0.5}Fe_2O_4$ nanoparticles, which are superparamagnetic[8] below 30 nm, in order to achieve linear and anhysteretic direct magnetoelectric effects in $Ni_{0.5}Zn_{0.5}Fe_2O_4$/P(VDF-TrFE) nanocomposites.

Experimental

P(VDF-TrFE) 75/25 mol % powder was purchased from Solvay Solexis, NZFO nanoparticles (10-30 nm) were purchased from Nanoamor and pure grade *N*,*N*-dimethylformamide (DMF) solvent was purchased from Fluka. NZFO/P(VDF-TrFE) 0-3 nanocomposites were prepared using the procedure described in [9]. NZFO nanoparticles were added to the DMF and the solution was placed in an ultrasonic bath

for 8 hours. P(VDF-TrFE) powder was subsequently added and the resultant solution was mixed using a Teflon mechanical stirrer and an ultrasonic bath until the polymer was completely dissolved (2 hours). Films were obtained by using a coating bar to spread the solution on a clean glass substrate. The solvent was evaporated by heating the films in an oven at 210 ºC for 10 minutes. Subsequent cooling to room temperature caused the polymer to crystallize. Finally, free-standing flexible polycrystalline films were obtained by detaching the glass substrate. Films of thicknesses ~ 25, 50 and 75 μm were prepared with nanoparticle content varying from 3 to 45 wt. % (0.01 to 0.23 volume fraction).

Results and Discussion

Ferroelectric $P(E)$ loops were measured using a Radiant Ferroelectric Premier II LC. Out-of-plane piezoelectric coefficients d_{33} were measured using a model 8000 wide range d_{33}-meter (APC Int Ltd). Prior to d_{33} measurements, the films were corona poled for 30 minutes at 120 ºC and during the subsequent cooling to room temperature. In-plane Young's modulus values E_Y were obtained from the initial slope of strain-stress curves measured for 3.5 mm × 13 mm specimens using a MINIMAT universal testing machine (Polymer Laboratories) in tensile mode, with a $2\ \text{mm min}^{-1}$ loading rate. Magnetization $M(H)$ curves were measured up to 18 kOe using a vibrating sample magnetometer (Oxford Instruments). For direct magnetoelectric measurements, poled nanocomposite films were cut into square specimens (side l ~ 6 - 10 mm), and circular 1.4 mm-diameter gold electrodes were sputtered on opposite sides. An electromagnet was used to provide H_{dc} bias, and a Helmholtz coil connected to an HP3245A source was used to generate the ac field H_{ac}. Dynamic magnetoelectric voltages were measured

using a 5302 EG&G lock-in amplifier. All measurements were carried out at room temperature.

Figure 1(a) shows room-temperature ferroelectric $P(E)$ loops of 50 μm-thick NZFO/P(VDF-TrFE) nanocomposites for selected compositions. The addition of small quantities of NZFO nanoparticles increases the remanent polarization P_r and piezoelectric coefficient $-d_{33}$ [Figure 1(b)] because nanoparticles improve the crystallinity of the polymer matrix near the interface[10,11]. For NZFO concentrations higher than 7 wt. %, the ferroelectric polarization decreases with increasing nanoparticles content and at 20 wt. % becomes smaller than the polarization of pure P(VDF-TrFE) due to the disruption of the polymer matrix[7]. 25 μm and 75 μm-thick nanocomposite films possess similar ferroelectric properties (not shown), unlike pure P(VDF-TrFE) thin films whose ferroelectric properties are strongly thickness dependent, e.g. due to changes in crystallinity and domain structure[12,13].

Figure 2 shows room-temperature out-of-plane magnetization $M(H)$ loops of 50 μm-thick NZFO/P(VDF-TrFE) nanocomposites for selected compositions. As expected, nanocomposite magnetization increases with increasing NZFO content. The nanocomposites show negligible magnetic coercivity and remanence, and the magnetization does not quite saturate at our maximum applied magnetic field of 18 kOe, consistent with the superparamagnetic behaviour[8] of nanoparticles whose diameter is less than 30 nm. Additional in-plane $M(H)$ measurements (not shown) evidenced the isotropic magnetic character of the composite films, confirming good nanoparticle dispersion. $M(H)$ measurements of 75 μm-thick films (not shown) revealed no dependence of magnetic properties on nanocomposite thickness.

Figure 3(a) shows that the magnetoelectric voltage coefficient α_{33} measured at resonance varies as a linear and anhysteretic function of out-of-plane bias field H_{dc}, for several different ferrite concentrations (the first index in α_{ij} indicates the collinear ferroelectric poling and electrical measurement directions, and the second indicates the applied magnetic field direction). The resonant frequency for each concentration was determined from 100 - 100 kHz scans at constant H_{dc} = 5 kOe [Figure 3(b)]. A peak in $\alpha_{33}(f)$ is seen at ~ 40 kHz for all the composites, and corresponds to the expected longitudinal electromagnetic resonance governed by the formula[14] $f_n \approx n/2l\sqrt{E_Y/\rho}$, where l is the length along the resonant direction, n is the order of the harmonic mode, and ρ and E_Y are density and Young's modulus, respectively (Table I). The observed linear behaviour of the magnetoelectric voltage coefficient may be attributed to linear magnetostriction in our nanocomposites, which has been previously reported at fields < 20-30 kOe in 0-3 composites comprising ferromagnetic particles in a silicone matrix with low concentration of magnetic particles[15], and also in some paramagnetic materials[16]. Note that varying the amplitude of H_{ac} from 0.4 – 1.5 Oe yielded a linear variation in magnetoelectric voltage (not shown) and therefore did not change α_{33}.

Magnetoelectric performance is maximised for wt. 15% of NZFO [Figures 3(a-c)]. As expected and predicted by the theoretical calculations, higher NZFO concentrated samples do not result in higher magnetoelectric coupling due to relative decrease of the piezoelectric phase within the composite[7]. In a similar way, note that maximum magnetoelectric performance is not obtained for the nanocomposite with the largest piezoelectric coefficient (wt. 7% of NZFO) because magnetoelectric effect is a product property and magnetization, and therefore magnetostriction, of the nanocomposite

increases with increasing NZFO content. The maximum value of $\alpha_{33} = 1.35$ mV cm^{-1} Oe^{-1} is smaller than the maximum $\alpha_{33} = 40$ mV cm^{-1} Oe^{-1} observed[7] in $CoFe_2O_4$/P(VDF-TrFE) and the maximum 16 mV cm^{-1} Oe^{-1} predicted[17] for $NiFe_2O_4$/P(VDF-TrFE) 0-3 nanocomposites, but larger than the 0.4 - 0.7 mV cm^{-1} Oe^{-1} response of all-ceramic 3-3 composites (Ni,Zn)Fe_2O_4/(Ba,Pb)(Zr,Ti)O_3 [18,19].

Figure 3(d) shows α_{33} together with α_{32} and α_{31}, as functions of H_{dc}, for the optimal sample with 15 wt. % of NZFO at resonance. The magnetoelectric response is reduced by a factor of around 3 when the dc bias field is applied in-plane, i.e. $\alpha_{33} \sim 3\alpha_{32} \sim 3\alpha_{31}$. Given that the magnetic properties are isotropic (Figure 2), this anisotropy is attributed to the piezoelectric response of the polymer, which for highly crystalline pure films of P(VDF-TrFE) obeys[20] $-d_{33} \sim 3d_{31} \sim 3d_{32}$.

Conclusions

To conclude, we studied the ferroelectric, piezoelectric, magnetic and direct magnetoelectric properties of free-standing, flexible 0-3 nanocomposite films of NZFO and P(VDF-TrFE) that were processed at low-temperature. Direct magnetoelectric effects up to 1.35 mV cm^{-1} Oe^{-1} were obtained in a 5 kOe dc field, for samples with 15 wt. % of NZFO at the 40 kHz resonance. NZFO/P(VDF-TrFE) nanocomposites improve upon $CoFe_2O_4$/P(VDF-TrFE) nanocomposites[7] as they show linear and non-hysteretic direct magnetoelectric responses up to 5 kOe. Our findings may be useful for dc magnetic-field sensors.

Acknowledgements

This work was supported by FEDER "Programa Operacional Factores de Competitividade – COMPETE" (NANO/NMed-SD/0156/2007) and Fundação para a Ciência e a Tecnologia FCT (PTDC/CTM/69316/2006). P. M. acknowledges support from FCT (SFRH/BD/45265/2008). X. M. acknowledges support from the Herchel Smith Fund. L. C. P. acknowledges support from the Engineering and Physical Sciences Research Council (EPSRC).

References

1. W. Eerenstein, N. D. Mathur and J. F. Scott, *Nature* **442**, 759 (2006).

2. M. Fiebig, J. *Phys. D-Appl. Phys.* **38**, R123 (2005).

3. C. W. Nan, M. I. Bichurin, S. Dong, D. Viehland and G. Srinivasan, *J. Appl. Phys.* **103**, 031101 (2008).

4. J. Ma , J. Hu , Z. Li and C. W. Nan, *Adv. Mater.* **23**, 1062 (2011).

5. J. Zhai, S. Dong, Z. Xing, J. Li and D. Viehland, *Appl. Phys. Lett.* **89**, 083507 (2006).

6. S. X. Dong , J. Y. Zhai , J. F. Li and D. Viehland, *Appl. Phys. Lett.* **89**, 252904 (2006).

7. J. X. Zhang, J. Y. Dai, L. C. So, C. L. Sun, C. Y. Lo, S. W. Or and H. L. W. Chan, *J. Appl. Phys.* **105**, 054102 (2009).

8. A. S. Albuquerque, J. D. Ardisson, W. A. A. Macedo and M. C. M. Alves, *J. Appl. Phys*. **87**, 4352 (2000).

9. P. Martins, C. M. Costa and S. Lanceros-Mendez, *Appl. Phys. A* **103**, 233 (2011).

10. B. Chu, M. Lin, B. Neese, X. Zhou, Q. Chen and Q. M. Zhang, *Appl. Phys. Lett.* **91**, 122909 (2007).

11. J. Li, S. Seok, B. Chu, F. Dogan, Q. Zhang and Q. Wang, *Adv. Mater*. **21**, 217 (2009).

12 .F. Xia, H. Xu, F. Fang, B. Razavi, Z. Y. Cheng, Y. Lu, B. Xu and Q. M. Zhang, *Appl. Phys. Lett.* **78**, 1122 (2001).

13. H. Xu, *J. Appl. Polym. Sci.* **80**, 2259 (2001).

14. C. Israel, V. M. Petrov, G. Srinivasan and N. D. Mathur, *Appl. Phys. Lett.* **95**, 072505 (2009).

15. S. Bednarek, *J. Magn. Magn. Mater*. **301**, 200 (2006).

16. E. Fawcett and G. K. White, *J. Appl. Phys.* **39** 576 (1968).

17. C. K. Wong and F. G. Shin, *J. Appl. Phys.* **102**, 063908 (2007).

18. B. K. Bammannavar and L. R. Naik, *J. Magn. Magn. Mater*. **321**, 382 (2009).

19. R S Devan, C M Kanamadi, S A Lokare and B K Chougule, *Smart Mater. Struct.* **15**, 1877 (2006).

20. H. Wang, Q. M. Zhang, L. E. Cross and A. 0. Sykes, *J. Appl. Phys.* **74**, 3394 (1993).

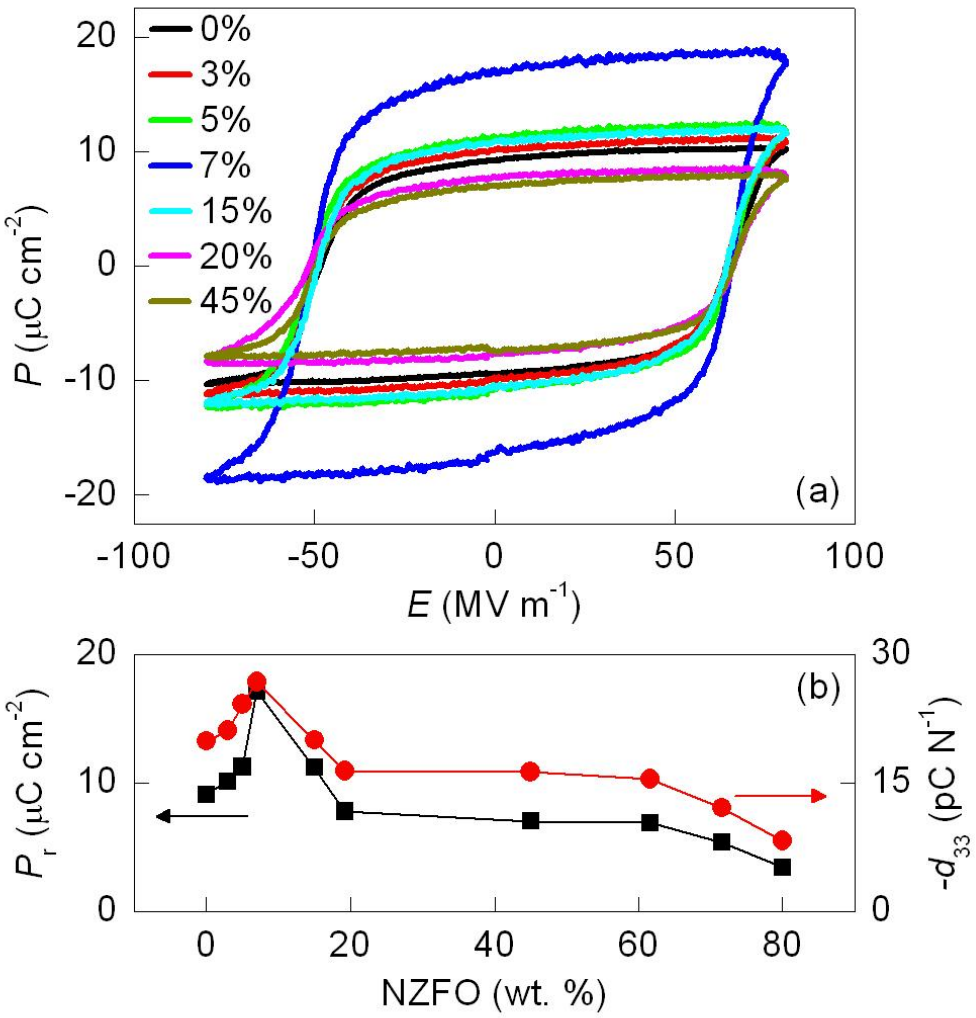

Figure 1. Room-temperature ferroelectric and piezoelectric properties of 50 μm-thick NZFO/P(VDF-TrFE) 0-3 nanocomposites. (a) Polarization *P* as a function of electric field *E* for composites with different ferrite concentrations. (b) Remnant polarization P_r and negative piezoelectric coefficient $-d_{33}$ as functions of NZFO content.

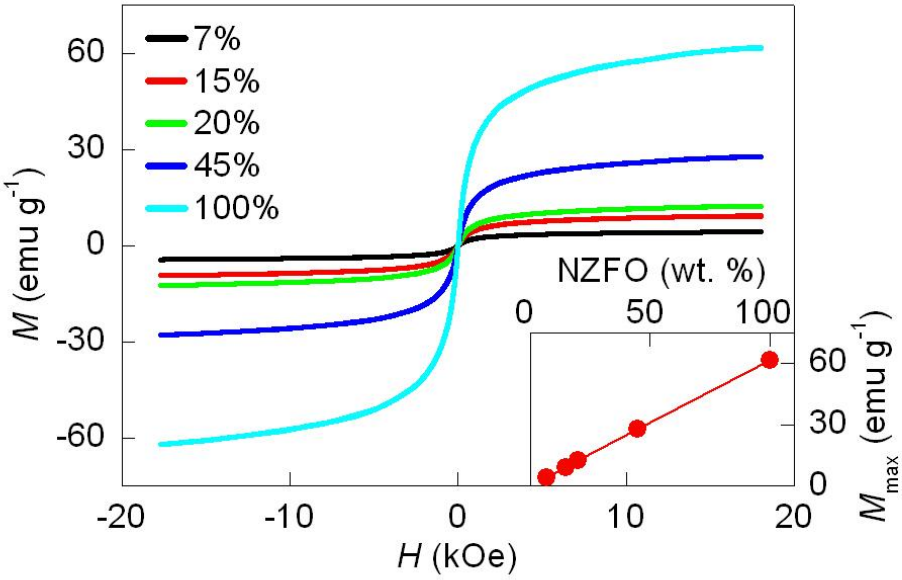

Figure 2. Room-temperature out-of-plane magnetization $M(H)$ of 50 μm-thick NZFO/P(VDF-TrFE) 0-3 nanocomposites with different ferrite concentrations. Inset shows the magnetization M_{max} measured at 18 kOe as a function of NZFO content.

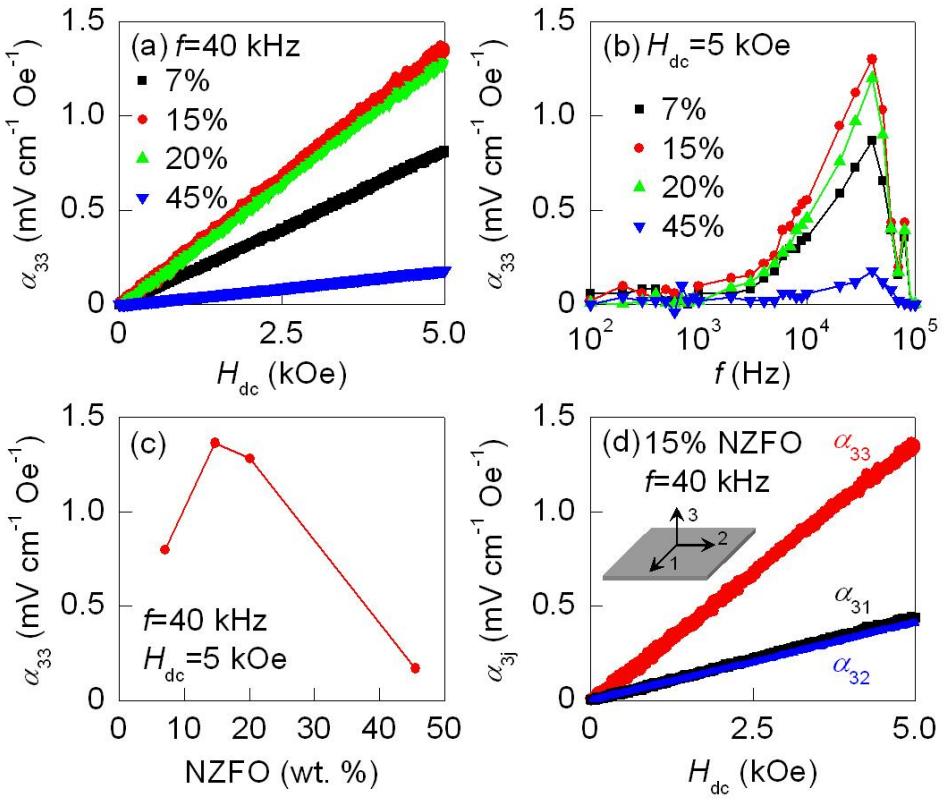

Figure 3. Room-temperature dynamic magnetoelectric response of 50 μm-thick NZFO/P(VDF-TrFE) 0-3 nanocomposites to out-of-plane H_{ac} fields of magnitude 1.27 Oe. (a) Magnetoelectric voltage coefficient α_{33} as a function of H_{dc} at resonance and (b) as a function of frequency at H_{dc} = 5 kOe . (c) Maximum value of α_{33} as a function of NZFO content. (d) α_{3j} as a function of H_{dc} magnitude and direction (inset) at resonance for the sample with 15 wt. % NZFO. In (a) and (d), magnetoelectric voltage is plotted for both increasing and decreasing H_{dc}.

NZFO content (wt. %)	Volume fraction (%)	ρ (kg m^{-3})	E_Y (GPa)	l (mm)	f (kHz)
7	2.7	1990	0.52	6	42.5
15	6.1	2100	1.06	9	39.5
20	8.4	2180	1.14	9	40.2
45	23	2660	1.50	10	37.6

Table I. Longitudinal resonant frequencies for 50 μm thick NZFO/P(VDF-TrFE) 0-3 nanocomposites with different ferrite concentration, computed from $f \approx (1/2l)\sqrt{E_Y/\rho}$. Volume fraction and density of the nanocomposites were calculated from the density of the components [1900 kg m^{-3} and 5200 kg m^{-3} for P(VDF-TrFE) and NZFO, respectively]. In-plane Young's modulus values E_Y of the composite films were obtained from the initial slope of strain-stress curves (not shown).